International Journal of Research Publication and Reviews

Journal homepage: www.ijrpr.com ISSN 2582-7421

Use of Fuzzy Logic Controller for Integration of Grid Connected Solar PV with Battery Storage System

Nikita Anilkumar Sonkamle[1], Prof. Sunil M Kulkarni[2]

[1]*ME (EPS) PESCOE, Nagsenvana, 431002 Aurangabad*
[2]*Associate Professor at PESCOE, Nagsenvana, 431002 Aurangabad*

A B S T R A C T

In this paper, a novel configuration of a three-level neutral-point-clamped (NPC) inverter that can integrate solar photovoltaic (PV) with battery storage in a grid-connected system I proposed. The strength of the proposed topology lies in a novel extended unbalance three-level vector modulation technique than can generate the correct ac voltage under unbalanced dc voltage conditions. This paper presents the design philosophy of the proposed configuration and the theoretical framework of the proposed modulation technique. A new control algorithm for the proposed system is also presented in order to control the power deliver between the solar PV, battery, and grid, which simultaneously provides maximum power point tracking (MPPT) operation for the solar PV. The effectiveness of the proposed methodology is investigated by the simulation of several scenarios, including battery charging and discharging with different levels of solar irradiation. The proposed methodology and topology is further validated using an experimental setup in the laboratory.

Keywords:Solar PV, unbalanced voltages, three level inverter, pulse width modulation, fuzzy Logic Control, solar irradiance

1. Existing System

1.1 Integration of Solar PV And Battery Storage

A circuit for integrating solar PV and battery storage has been proposed. Using a Three-Level Inverter with an Improved Unbalanced DC Functionalist Based on the talks in Sections I and II, two new configurations of a three-level inverter to integrate battery storage and solar PV are proposed in Fig. 6, with no additional converter needed to connect the battery storage to the grid-connected PV system. These can help lower costs and increase overall system efficiency, especially in medium and high-power applications.The basic arrangement is depicted in Fig.1(a). The proposed method allows power from a renewable energy source to be delivered to the grid while also permitting charging and discharging of the battery storage system as desired by the control system. The suggested system will be able to regulate the total of the capacitor voltages (VC1+VC2 =Vdc) to achieve the MPPT condition while also controlling the lower capacitor voltage (VC1) to control the charging and discharging of the battery storage system separately. Furthermore, even with unbalanced capacitor voltages on the dc side of the inverter, the output of the inverter can still have the correct voltage waveform with minimal total harmonic distortion (THD) current in the ac side.

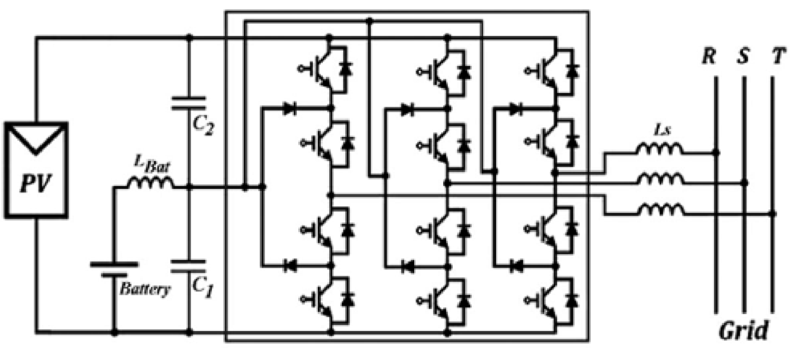

(a)

* *Nikita Sonkamle*
E-mail address: snikky1218@gmail.com

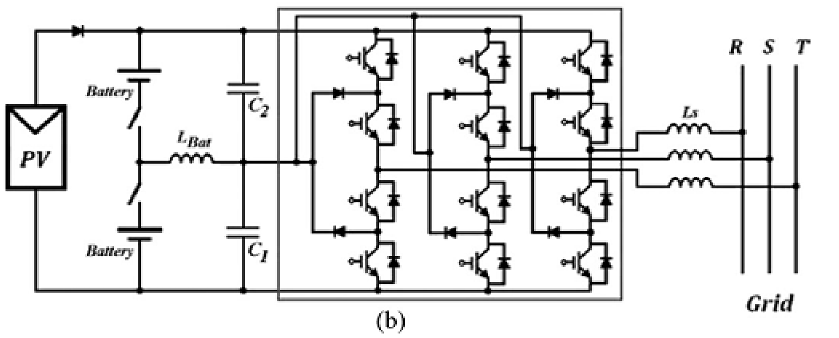

Figure.1: integrating solar PV and battery storage:(a) basic configuration,(b) improved configuration.

Although this setup can work in most situations, the system cannot function effectively with just one battery when the sola PV does not produce any electricity. Figure 1(b) depicts the revised setup, which now connects two batteries to two capacitors via two relays. When one of the relays is closed and the other is open, the configuration in Fig.1(b) is similar to that in Fig.1(a), which allows the renewable energy source to provide power while charging or discharging the battery storage. When renewable energy is not available, however, both relays can be closed, allowing the dc bus to transport or absorb active and reactive electricity to and from the grid. It's worth noting that these relays can be turned on or off as needed; no PWM control is necessary. This also allows you to choose which of the two batteries to use.

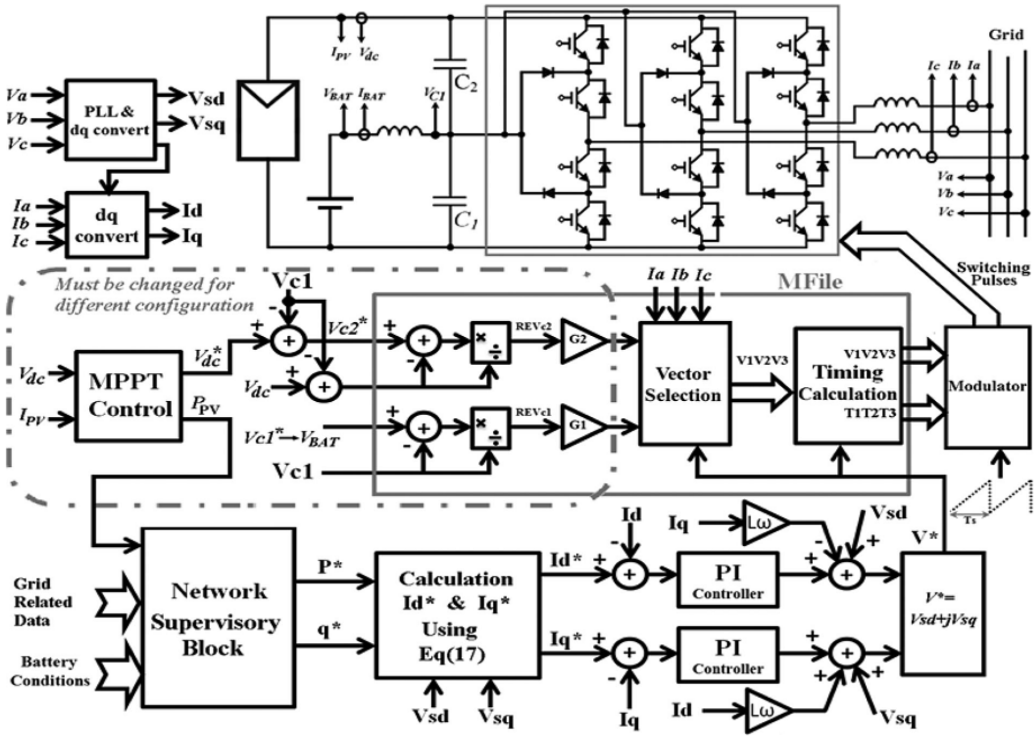

Figure.2: control system diagram to integrate PV and battery storage

1.2. Description of Control System

Three distinct relay configurations are shown in Figure2: 1) when the top relay is closed, 2) when the bottom relay is closed, and 3) when both relays are closed. The control system for configuration 1) is depicted in block diagram form in Fig. 2. The network supervisory block will determine the inverter's requested active and reactive power generation to be delivered to the grid in Fig. 2. Based on the available PV generation, grid data, and current battery variables, this will be accomplished.To accomplish the MPPT condition, the MPPT block finds the requested dc voltage across the PV. This voltage can be estimated by employing a slower-dynamic control loop and a measurement of the available PV power. [3] and [4] provide more information on the MPPT algorithm for determining the desired voltage (V dc). The requested inverter current in the dq-axis,id and iq, can be calculated using (17): based on the requested active()and reactive power(q), and the grid voltage in the dq-axis, vsd and vsq, and the grid voltage in the dq-axis, vsd and vsq. $\begin{cases} p = \upsilon_{sd} i_d + \upsilon_{sq} i_q \\ q = \upsilon_{sq} i_d + \upsilon_{sd} i_q \end{cases} \Rightarrow$

$$i_d^* = \frac{p^* \upsilon_{sd} - q^* \upsilon_{sq}}{\upsilon_{sd}^2 + \upsilon_{sq}^2}; \quad i_q^* = \frac{q^* \upsilon_{sd} - p^* \upsilon_{sq}}{\upsilon_{sd}^2 + \upsilon_{sq}^2} \quad (17)$$

The inverter desired voltage vector can be calculated using a proportional and integral (PI) controller and a decoupling control structure. Figure 2 depicts the suggested control system. The battery will be charged using surplus energy from the PV or discharged to support the PV when the available energy cannot support the needed power in the proposed system to transfer a set amount of power to the grid.

The relevant sector in the vector diagram can be found after analysing the requested reference voltage vector. The relative errors of capacitor voltages reported in (18) and (19) are utilised to determine which short vectors should be chosen.

$$ev_{c1} = \frac{V^*{}_{C1} - V_{C1}}{V_{C1}} \quad (18)$$

$$ev_{c2} = \frac{V^*{}_{C2} - V_{C2}}{V_{C2}} \quad (19)$$

Where V ∗ C1 and V ∗ C2 are the desired capacitor voltages, andVC1 andVC2 are the actual capacitor voltages for capacitorC1 and C2, respectively.

The short vectors will determine whether the capacitor will be charged or discharged. The relative mistakes of capacitor voltages and their effectiveness on control system behaviour are significant in determining which short vector should be chosen. Based on this concept, a decision function "F" can be defined, as shown in (20).

$$F = G_1 ev_{cl} - G_2 eV_{c2} \quad (20)$$

where G1 and G2 are the gains associated with each of the capacitor voltages' relative errors. G1 and G2 are utilised to decide whether relative capacitor voltage error is more critical, allowing for greater control of the chosen capacitor voltage. For example, in a traditional three-level inverter where the capacitor voltages must be balanced, G1 and G2 must have the same value with equal reference voltage values, but in the proposed application where the capacitor voltages can be unbalanced, G1 and G2 must be different and their values are completely dependent on their definitions of desired capacitor voltages. PV can be adjusted to the MPPT and C1 voltage can be managed to allow charging and discharging of the battery by using VC2 =VdcVC1 and VC1 =VBAT and selectingG2much greater thanG1.

The sign off is used to indicate which short vectors should be chosen at each time step. When F is positive, short vectors that can chargeC1 or dischargeC2 in that particular time step must be chosen using (14) and reasoning similar to (15) and (16). (16). When F is negative, the short vectors that can chargeC2or dischargeC1 in that particular time step must be chosen.

On the ac side, the inverter will generate the requested active power, p, and reactive power, q, by implementing the requested voltage vector and applying the right time of the applied vectors, as shown in the control system diagram in Fig. 2. MPPT control can also be done on the dc side by stringent control ofVC2 (G2 G1) with a reference value of (V dcVC1) and more flexible control ofVC1 with a reference value of the battery voltage, VBAT. The suitable short vectors to apply to construct the requested vector can be identified by utilising the decision function (F) with the given reference values. The PV arrays may transmit the maximum available power (PPV) using MPPT control, and the requested power p is transferred to the grid by generating the requested vector on the ac side. The control system will then controlVC1 to transfer excess power (PPVP) automatically.

Configuration 2) uses the identical control mechanism, but the capacitors' generated reference voltages are changed. Configuration 3) depicts two storage systems that are connected to the grid but do not contribute any PV power, such as at night when the PV is not providing any output power.

2. Proposed System

2.1 Introduction to Fuzzy Logic Control

A mathematical method for coping with uncertainty is fuzzy logic. It provides a soft computing alliance that emphasises the importance of computing with language. The following are the primary characteristics of FLC:

- A fuzzy logic design programme that allows you to create fuzzy inference systems and see and analyse the results.
- Fuzzy interference systems can be created using membership functions.
- User-defined rules can use AND, OR, and NOT logic.

- Neuron adaptive and fuzzy clustering learning approaches automate the shaping of membership functions.
- Possibility of incorporating a fuzzy interface system into a simulation model.

2.2 Working with the Fuzzy Logic Control

- Develop and analyze fuzzy inference systems
- Develop adaptive neuro fuzzy inference systems
- Perform fuzzy clustering

2.3 Building a Fuzzy Inference System

Fuzzy inference is a method that interprets the values in the input vector and based on user defined rules, assigns values to the output vector. The following editors and viewers are provided

- **FIS editor**:-Displays general information about a fuzzy inference system.
- **Membership function:**-Lets you display and edit the membership functions associated with the input and output variables of the FIS.
- **Rule editor**:-Lets you view and edit fuzzy rules using one of three formats: like syntax, concise symbolic notation, or an indexed notation.
- **Rule viewer**:-Lets you view detailed behavior of a FIS to help diagnose the behavior of specific rules or study the effect of changing input variables.
- **Surface viewer**:-Generates a 3-D surface from two input variables and the output of an FIS.

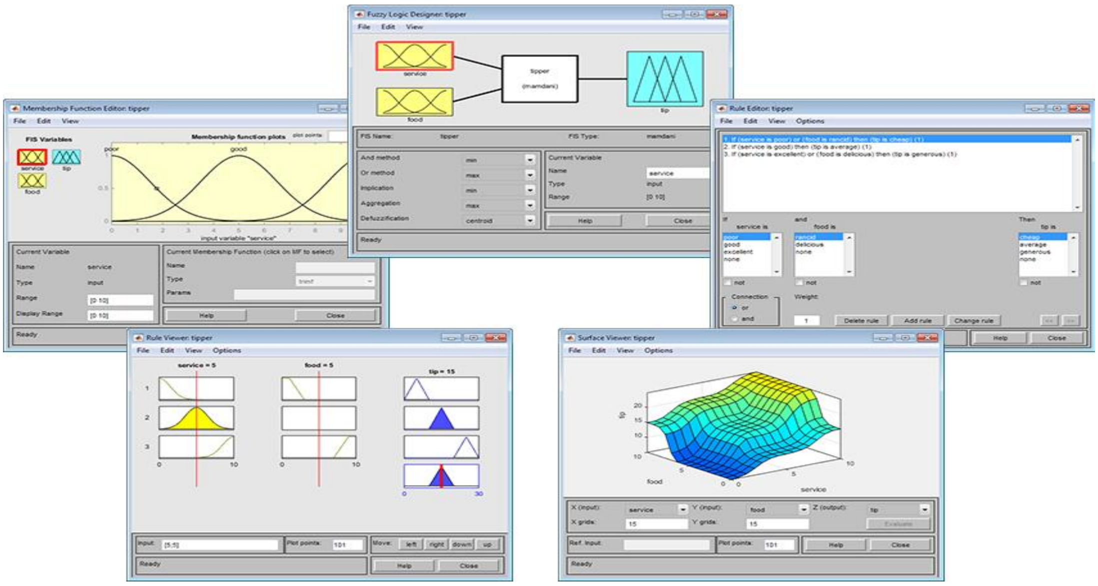

Figure 3: The Membership Function Editor (top left), FIS Editor (center), Rule Editor (top right), Rule Viewer (bottom left), and Surface Viewer (bottom right).

2.4 Simulating and Deploying Fuzzy Inference Systems.

The fuzzy logic controller block in a simulink model of your system can be used to evaluate FIS performance. For most fuzzy inference systems, the fuzzy logic controller block generates a hierarchical block diagram representation automatically. There have been a variety of methods used to track the maximum power point, but this work introduced a fuzzy controller to track the MPP of a PV system. Engineers use fuzzy logic to deal with uncertainty by assigning degrees of certainty to the answer to a logical query. Fuzzy logic has been used successfully in the commercial world to control machinery and consumer products. Fuzzy logic systems are easy to develop and understand, even for those who aren't experts in control theory. In the realm of MPPT, another advantage of these controllers is that their output has low oscillations and quickly converges around the intended MPP.

Furthermore, they have performed admirably in the face of abrupt irradiation fluctuations. The duty cycle (D) of the switching signal is controlled using the proposed algorithm. The suggested fuzzy controller includes two inputs: PV system power (P) and PV voltage change (V). Fuzzification, inference, and finally defuzzification are the three steps of a fuzzy logic controller. It was decided to utilise membership functions with a triangle shape. There has been constructed a Mamdani-type system with two inputs and one output. Based on simulated data, the signal range has been established. The input signals are classified into five categories in this study: Very Low (VL), Low (L), Medium (M), High (H), and Very High (VH) (VH). The relationship between output power and ideal duty cycle values is used to determine subsets of the membership functions. In this study, output power of the PV system was calculated, as well as ΔV of the system at different cases of partial and full shading. The range of them was found to represent the range of the input membership functions. The relation between them with the duty cycle was studied to determine the subsets and the rules of the fuzzy controller.

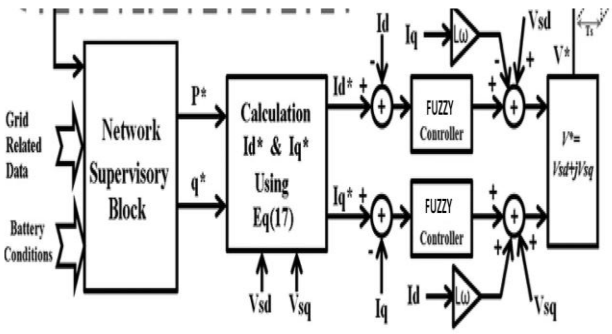

Figure 4: fuzzy controller used in control system

Instead of a PI controller, a fuzzy logic controller is employed. The fuzzy logic controller (FLC) is a relatively new controller that manages the dc-link voltages with ease. When compared to a PI controller, this controller is more versatile. There are no mathematical computations required

3. Simulation Results

3.1 Simulation and Validation of the Proposed Topology and Control System

To test the effectiveness of the suggested topology and control system, simulations were run using MATLAB/Simulink. The inverter is connected to the grid via an LCL filter. The block diagram of the simulated system is shown in Figure 8.

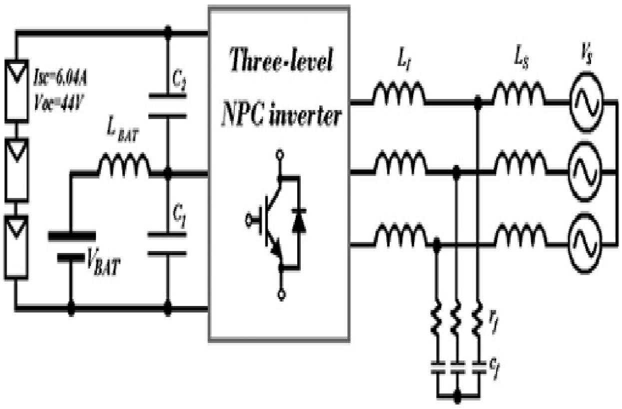

Figure 5: Block diagram of the simulated system.

Table 1: parameters of the simulated system

V_{BAT}	Vs (line)	L_{BAT}	C_1,C_2	L_1	L_s
60 V	50 V	5 mH	1000 uF	500 uH	900 uH
r_f	C_f	K_p	K_i	G_1	G_2
3 Ω	14 uF	2.9	1700	1	200

Three, series-connected PV modules are used in the simulation. The mathematical model of each of the PV units is given in below equation and used in the simulation

$$Ipv = I_{SC} - 10^{-7}\left(e^{\left(\frac{V_{PV}}{2574\times10^{-3}}\right)} - 1 \right) \quad (21)$$

Where ISC is the short circuit current of the PV.

ISC is considered to alter with varied irradiances in the simulation. With a solar irradiation of 1000 W/m 2, ISC equals 6.04 A, and the PV panels' open circuit voltage equals VoC =44V. Table I lists the major parameters of the simulated system.G2 must be substantially greater than G1 in order to accomplish the MPPT condition and have the flexibility to charge and discharge the battery, as previously stated. According to our tests, any figure more than 100 is good for this ratio. Increasing the G2/G1 ratio, on the other hand, will have no effect on other results because it only affects short-vector selection. As stated in Table I, this value was chosen to be 200 in order to have strong control over Vdc.The purpose of the LBAT is to smooth out the battery current, especially when it is transitory. The inductor value can be set to a broad range of values; however, lowering it will increase the battery's current overshoot. Its value is also influenced by the value of the nearby capacitor and the transient voltages. The value of LBAT is preferred to be low due to practical concerns (such as size and cost), and has been chosen to be 5 mH based on our simulation tests.

Modelling the system in the dq-frame is used to choose the values of Kp and Ki. Using the decoupling technique presented in Fig 6, the existing control loop can be changed to a simple system. [22] has the specifics of this approach. Two separate scenarios have been simulated for theoretical purposes to explore the effectiveness of the suggested topology and control algorithm when the reference inputs are changed in a stepwise manner under the following conditions:The effect of a step change in the requested active and reactive power to be transferred to the grid when the solar irradiance is assumed to be constant.. The effect of a step change of the solar irradiation when the requested active and reactive power to be transmitted to the grid is assumed to be constant.

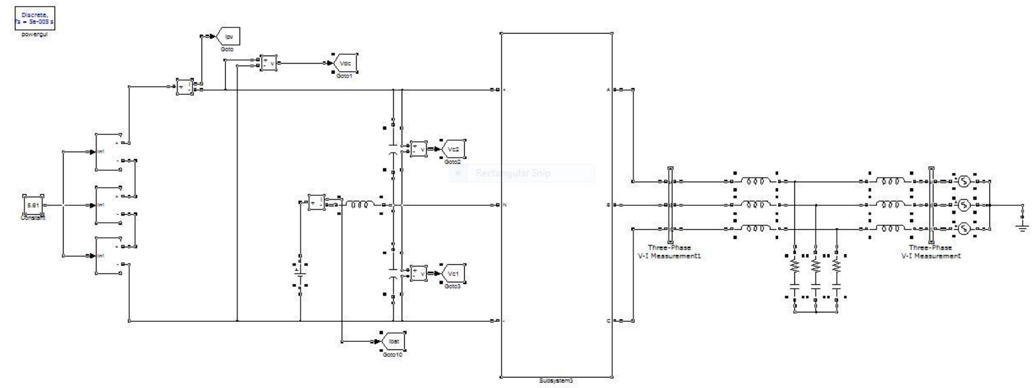

Figure 6: simulation circuit

When working with a low precision microprocessor system, a slope controlled change in the reference input is frequently employed rather than a step change to lessen the chance of mathematical internal calculation errors and also to prevent the protection mechanism from activating. Furthermore, in real-world settings, the inputs to the systems, such as sun irradiation, do not alter instantly as a step change. The suggested system is simulated utilising a slope controlled variation in the requested active power to be transferred to the grid while the solar irradiation is assumed to be constant with this practical application in mind. To verify this, a laboratory test employing the identical scenario is conducted, and the experimental results in Section V can be compared to the simulation results

3.1 First Scenario

In the first scenario, solar irradiation is expected to produce ISC=5.61A in the PV module, according to (21). The MPPT control block, illustrated in Fig. 7, determines the requested PV module voltageV dc, which is 117.3 V, in order to maximise the power generated by the PV system, which may generate 558 W of electrical power. At time t=40 ms, the requested active power to be sent to the grid is adjusted from 662 W to 445 W, while the reactive power changes from zero to 250 VAR at time t=100 ms.

The results of the first scenario simulation are shown in Figure indicate that the suggested control system correctly followed the requested active and reactive power, and Figure 3.4(c) illustrates that the PV voltage was accurately managed (to be 177.3 V) to get the maximum power from the PV module. When the grid power is more than the PV power, the battery discharges, and when the PV power is greater than the grid power, the battery charges. Because the power provided by the PV is insufficient, the battery discharges at 1.8 A before time t =40 ms, as shown in Fig. 9(d). The battery current is around –1.8 A after time t =40 ms, indicating that the battery is being charged from the PV module's additional power. Figures shows the grid-side currents with a THD less than 1.29% due to the LCL filter. The simulation results in Fig. 7 show that the whole system produces a very good dynamic response.

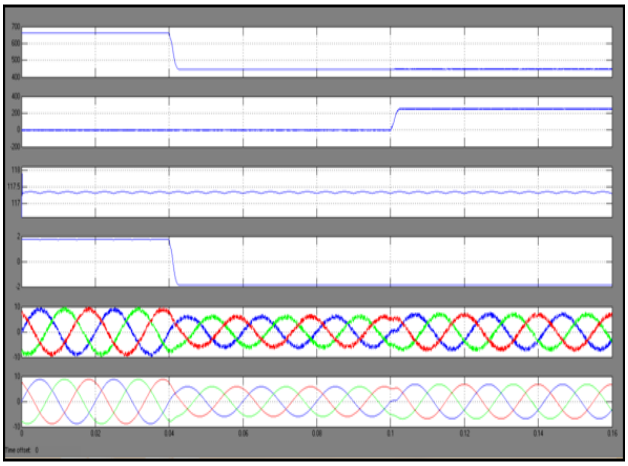

Figure 7: Simulated results for the first scenario. (a) Active power injected to the grid. (b) Reactive power injected to the grid. (c) PV module DC voltage. (d) Battery current. (e) Inverter AC current. (f) Grid current

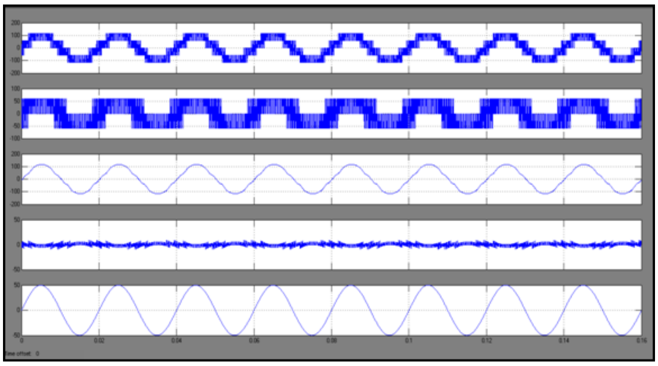

Figure 8 :Simulated inverter waveforms. (a) Vab-Phase to phase inverter voltage. (b) Vao-Inverter phase voltage reference to midpoint. (c) Filtered Von Filtered inverter phase voltage reference to midpoint. (d) Filtered Von-Filtered midpoint voltage reference to neutral. (e) Filtered Van-Filtered phase voltage reference to neutral.

3.2 Second Scenario

In the second scenario, it is expected that the solar irradiation will shift, resulting in ISC=4.8,4 and 5.61 A from the PV module. To get the most power from the PV units, which may provide 485, 404, and 558 W, the MPPT control block decides that Vdc must be 115.6, 114.1, and 117.3 V. During the simulation, the requested active power to be sent to the grid is kept constant at 480W, while the reactive power is kept at zero.

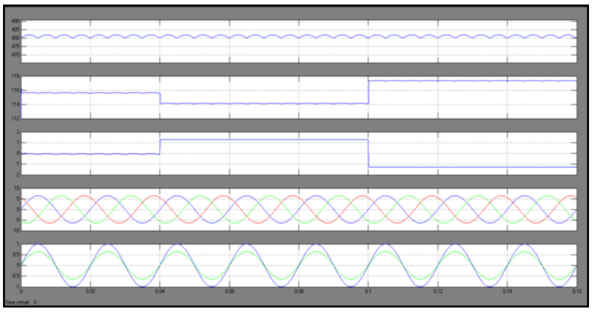

Figure 9: Simulated results for the second scenario. (a) Active power injected to the grid. (b) PV module DC voltage. (c) Battery currents. (d) Grid side currents. (e) Grid side Phase (a) voltage and its current.

Fig.: 9 shows the results of the second scenario simulation. Fig. 9 shows that the inverter is able to generate the requested active power. It shows that the PV voltage was controlled accurately for different solar irradiation values to obtain the relevant maximum power from the PV modules.The charging and draining of the battery are correctly conducted. The battery has augmented PV power generation in order to satisfy the grid's demand. The quality of the waveforms of the grid-side currents is satisfactory, as shown in Fig. 3.5(d), indicating that the suggested control approach generates the correct PWM vectors. The inverter can give a quick transient response by employing the recommended technique. The a-phase voltage and current of the grid, which are always in-phase, indicating that the reactive power is zero at all times.

3.3Third Scenario

In the third simulation, the desired active power to be sent to the grid is initially set at 295 W, then begins to decrease as a slope controlled change at time t=40 ms, eventually remaining constant at 165 W at time t=90 ms. According to ISC=2.89, solar irradiation will yield ISC=2.89 in the PV module (21). To accomplish MPPT condition, the requested PV module voltage V dc will be 112.8 V to create 305 W of electrical power.

Fig 10 shows that the active power transmitted to the grid reduces and follows the requested active power. Fig shows the battery current which is about 0.1 A before t=40 ms and then because of the reduced power transmission to the grid with a constant PV output, the battery charging current is increased and finally fixed at about 2.2 A. To meet the MPPT criteria, the dc voltage is kept at 112.8 V for this simulation. It is vital to note that the dc bus is imbalanced during the simulations because the battery voltage is equivalent to 60 V during the simulation, and so equal capacitor voltages are not possible in this case.

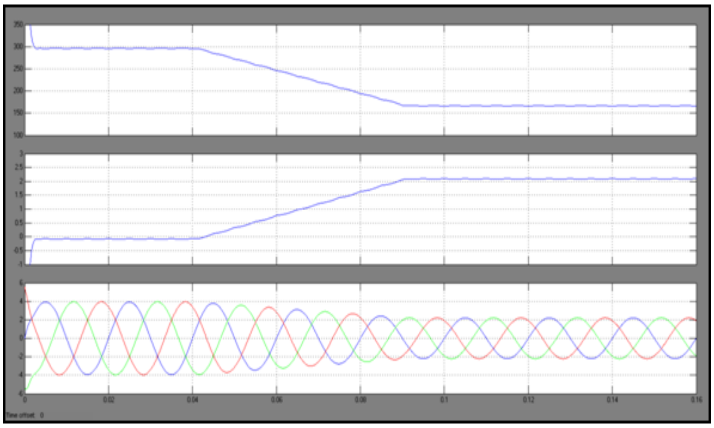

Figure 10:Simulated result for third scenario. (a) Active power injected to the grid. (b) Battery current. (c) Grid side currents

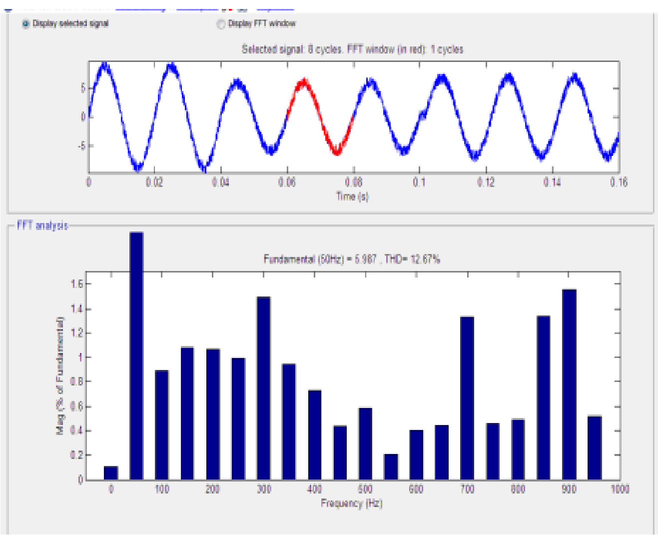

(a)

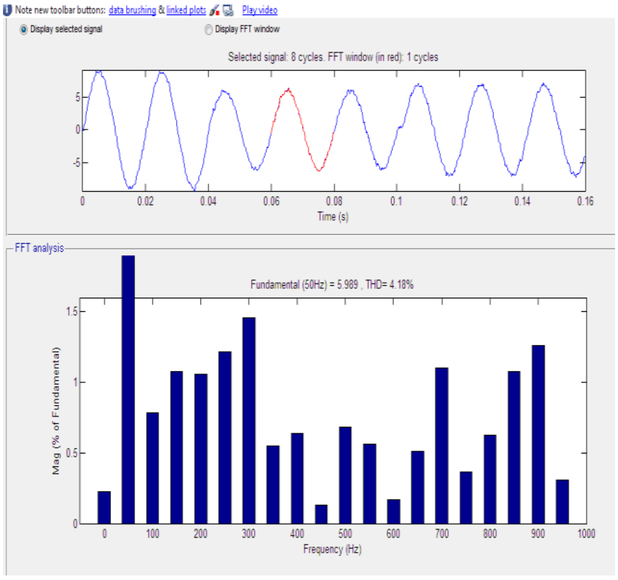

(b)

Figure 11:Total Harmonic Distortion of the Three Level NPC Output Current (a) Using PI Controller (b) Using Fuzzy Logic controller

4. Conclusion

On the dc side of the inverter, a three-level NPC voltage source inverter that can incorporate both renewable energy and battery storage has been demonstrated. It has been suggested a theoretical framework for a new extended unbalance three-level vector modulation technique that can generate the right ac voltage under unbalanced dc voltage conditions. In order to govern power flow between solar PV, battery, and grid system while MPPT functioning for the solar PV is achieved simultaneously, a new control algorithm for the proposed system has been provided. Simulations were used to assess the effectiveness of the suggested topology and control method, and the results are provided. The results show that the suggested system can control ac-side current, as well as battery charging and discharging currents, at various solar irradiation levels. The proposed topology for controlling both PV and battery storage in supplying electricity to the ac grid has been validated by trials utilising a prototype developed in the lab.

REFERENCES

J. Zaragoza, J. Pou, S. Ceballos, E. Robles, C. Jaen, and M. Corbalan, “Voltage-balance compensator for a carrier-based modulation in the neutral-point-clamped converter,”IEEE Trans. Ind. Electron., vol. 56, no. 2, pp. 305–314, Feb. 2009.

W. Chenchen and L. Yongdong, “Analysis and calculation of zerosequence voltage considering neutral-point potential balancing in threelevelnpcconverters,”IEEE Trans. Ind. Electron., vol. 57, no. 7, pp. 2262– 2271, Jul. 2010.

S. Busquets-Monge, S. Somavilla, J. Bordonau, and D. Boroyevich, “Capacitor voltage balance for the neutral-point-clamped converter using the virtual space vector concept with optimized spectral performance,”IEEE Trans. Power Electron., vol. 22, no. 4, pp. 1128–1135, Jul. 2007.

S. Busquets-Monge, J. Bordonau, D. Boroyevich, and S. Somavilla, “The nearest three virtual space vector PWM—A modulation for the comprehensive neutral-point balancing in the three-level NPC inverter,”IEEE Power Electron. Lett., vol. 2, no. 1, pp. 11–15, Mar. 2004.

J. Pou, J. Zaragoza, S. Ceballos, M. Saeedifard, and D. Boroyevich, “A carrier-based PWM strategy with zero-sequence voltage injection for a three-level neutral-point-clamped converter,” IEEE Trans. Power Electron., vol. 27, no. 2, pp. 642–651, Feb. 2012.

J. Wei-dong, D. Shao-wu, C. Liu-chen, Y. Zhang, and Q. Zhao, “Hybrid
PWM strategy of SVPWM and VSVPWM for NPC three-level voltagesourceinverter,”IEEE Trans. Power Electron., vol. 25, no. 10, pp. 2607– 2619, Oct. 2010.

J. Zaragoza, J. Pou, S. Ceballos, E. Robles, P. Ibaez, and J. L. Villate, “Acomprehensive study of a hybrid modulation technique for the neutralpoint-clamped converter,”IEEE Trans. Ind. Electron., vol. 56, no. 2,pp. 294–304, Feb. 2009.

Z. Jian-Yong, S. Zhang-Liang, M. Jun, and L.-f. Wang, “An improved neutral-point voltage balancing algorithm for the npc three-level inverter based on virtual space vector PWM,” inProc. Int. Conf. Elect. Control Eng., Jun. 2010, pp. 3283–3287.

J. Pou, D. Boroyevich, and R. Pindado, “New feedforward space-vector PWM method to obtain balanced AC output voltages in a three-level neutral-point-clamped converter,”IEEE Trans. Ind. Electron., vol. 49,no. 5, pp. 1026–1034, Oct. 2002.

M. G. Villalva, J. R. Gazoli, and E. R. Filho, “Comprehensive approach to modeling and simulation of photovoltaic arrays,” IEEE Trans. PowerElectron., vol. 24, no. 5, pp. 1198–1208, May 2009.

A. Yazdani and R. Iravani,Voltage-Sourced Converters in Power Systems. New York, NY, USA: Wiley, 2010.